JCB Report

A role for cytoplasmic dynein and LIS1 in directed cell movement

Denis L. Dujardin,[1,2] Lora E. Barnhart,[1] Stephanie A. Stehman,[1] Edgar R. Gomes,[1] Gregg G. Gundersen,[1] and Richard B. Vallee[1]

[1]College of Physicians and Surgeons, Department of Pathology, and Department of Anatomy and Cell Biology, Columbia University, New York, NY 10032
[2]Ecole Supérieure de Biotechnologie de Strasbourg, Centre National de la Recherche Scientifique, UMR 7100, Parc d'Innovation, Boulevard Sébastien Brandt, BP 10413, 67412 ILLKIRCH Cedex, France

Cytoplasmic dynein has been implicated in numerous aspects of intracellular movement. We recently found dynein inhibitors to interfere with the reorientation of the microtubule cytoskeleton during healing of wounded NIH3T3 cell monolayers. We now find that dynein and its regulators dynactin and LIS1 localize to the leading cell cortex during this process. In the presence of serum, bright diffuse staining was observed in regions of active ruffling. This pattern was abolished by cytochalasin D, and was not observed in cells treated with lysophosphatidic acid, conditions which allow microtubule reorientation but not forward cell movement. Under the same conditions, using total internal reflection fluorescence microscopy, clear punctate dynein/dynactin containing structures were observed along the sides and at the tips of microtubules at the leading edge. Overexpression of dominant negative dynactin and LIS1 cDNAs or injection of antidynein antibody interfered with the rate of cell migration. Together, these results implicate a leading edge cortical pool of dynein in both early and persistent steps in directed cell movement.

Introduction

Cytoplasmic dynein is a molecular motor associated with diverse subcellular structures, such as membranous organelles and kinetochores, which it transports or pulls toward the minus end of microtubules. Two lines of recent evidence have implicated dynein in a new and potentially general role in directed cell movement. First, dynein interacts with the LIS1 protein (Faulkner et al., 2000; Sasaki et al., 2000; Smith et al., 2000) mutations in which cause lissencephaly, a disease resulting from incomplete migration of neural progenitor cells from the ventricular zone during early brain development (Reiner et al., 1993). A second line of evidence implicating dynein itself in cell movement has come from analysis of cytoskeleton reorganization in wounded monolayer cultures (Etienne-Manneville and Hall, 2001; Palazzo et al., 2001), a system which provides an excellent means for controlling the timing and direction of cell movement. An early step in wound healing involves the reorientation of the centrosome, the major microtubule organizing structure, to a position ahead of the nucleus and toward the leading cell edge (Gundersen and Bulinski, 1988). Microtubules located at the front of the cells also become preferentially stabilized, and the cells migrate to close the wound. Injection of antidynein antibody or overexpression of the dynactin subunit dynamitin each interfered with centrosome reorientation (Etienne-Manneville and Hall, 2001; Palazzo et al., 2001) without affecting microtubule stabilization or organization (Palazzo et al., 2001).

These data implicated dynein in the reorientation process. However, the mechanism by which dynein contributed to this behavior, and a possible direct role in cell translocation were not assessed. We now report that dynein, its associated regulatory complex dynactin, and LIS1 are enriched at the leading cell edge in wounded NIH3T3 fibroblast monolayers during MTOC reorientation and subsequent cell migration. Inhibition of dynein, dynactin, and LIS1 interfere not only with reoriention of the microtubule network, but also with persistent directed cell migration as well.

Address correspondence to Richard B. Vallee, Columbia University, College of Physicians and Surgeons, Dept. of Pathology and Anatomy and Cell Biology, P & S 15-409, 630 W. 168th St., New York, NY 10032. Tel.: (212) 342-0546. Fax: (212) 305-5498. email: rv2025@columbia.edu

Key words: microtubule; lissencephaly; motor protein; lamellipodia

Abbreviations used in this paper: LPA, lysophosphatidic acid; TIRF, total internal reflection fluorescence microscopy.

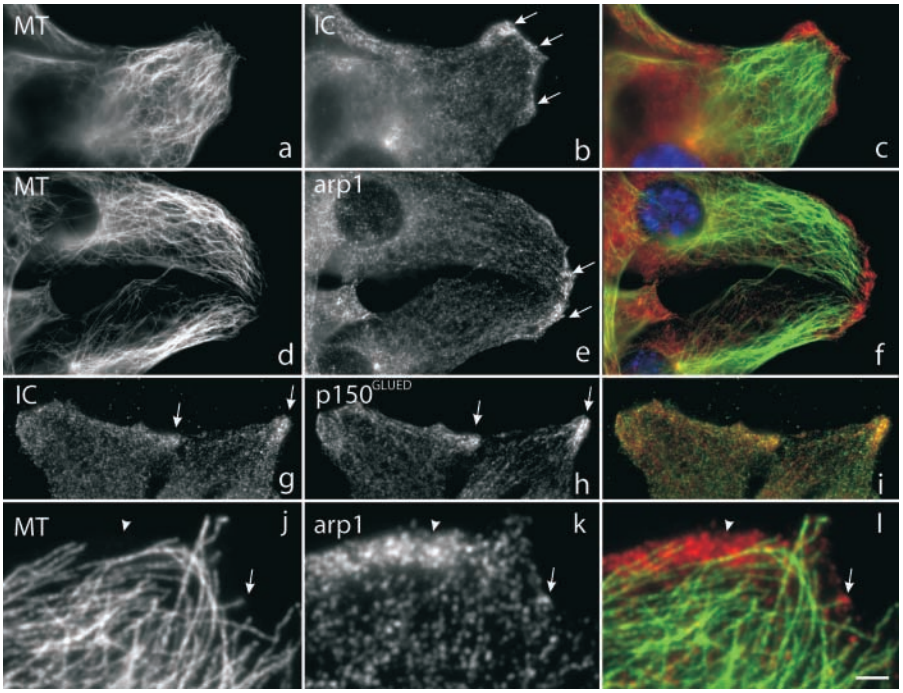

Figure 1. **Localization of dynein and dynactin during wound healing.** Immunofluorescence microscopy of wounded NIH3T3 cell monolayers. (a–c) double labeling showing antitubulin (MT), antidynein (IC), and merged staining pattern (dynein, red); (d–f) double labeling showing antitubulin (MT) and antidynactin (arp1) and merged image (dynactin, red). (g–i) labeling showing antidynein (IC) and antidynactin ($p150^{GLUED}$) and merged image (dynactin, red). (j–l) higher magnification view of double labeling showing antitubulin (MT) and antidynactin (arp1) and merged image (dynactin in red). Both diffuse (arrowheads), and punctate (arrows) staining can be observed. Cells were fixed 6 h or (g–i) 30 min after wounding. DAPI staining of nuclei is shown in blue. Bar: (a–i) 5 μm; (j–l) 2 μm.

Results and discussion

Localization of dynein and its related proteins during wound healing

To monitor the behavior of cytoplasmic dynein during cell migration, we performed immunofluorescence microscopy using antibodies to dynein or its accessory proteins. We detected a striking enrichment of dynein at the leading edge of the cell monolayer as the cells migrated to close the wound (Fig. 1, a–c, arrows; Fig. 2 j; Fig. 3 b). Dynactin, which has been implicated in dynein targeting (Echeverri et al., 1996) and processivity (King and Schroer, 2000) was also enriched at these sites (Fig. 1, d–f, arrows), where it colocalized with dynein (Fig. 1, g–i, arrows). In many cells, dynein and dynactin were enriched at regions toward which microtubules were directed (Fig. 1, a–f). Both punctate and diffuse staining were observed. The latter pattern could be seen even in regions containing few or no microtubules (Fig. 1, j–l, arrowheads). It was often observed in regions of lamellipodial protrusion as judged by the presence of membrane ruffles visualized by phase-contrast microscopy (Fig. 2, a–c arrows; and Fig. S1 A, available at http://www.jcb.org/cgi/content/full/jcb.200310097/DC1). The staining did not overlap precisely with the ruffles. Furthermore, in many cells, dynein and dynactin were enriched relative to the membrane marker CD44 (Fig. 2 m–o; Fig. S1, B and C; Perschl et al., 1995), and leading edge staining was clearly observed by confocal (Fig. S1 D) and total internal reflection fluorescence microscopy (TIRF; see Fig. 3).

Punctate dynein and dynactin staining was also observed throughout the cell, but was enriched at the leading edge of cells in the recovering wound. Some of these immunoreactive spots were associated with the ends of microtubules (Fig. 1, j–l, arrows). This pattern, however, was morphologically distinct from the elongated regions of dynein and dynactin seen at the plus ends of growing microtubules in vertebrate cells (Vaughan et al., 1999). Furthermore, antibodies such as the polyclonal anti-IC used in the current paper fail to produce the elongated patterns, and serve as selective markers for the cortical dynein structures observed here.

Actin and the cortical protein IQGAP1 (not depicted) were also enriched at sites of dynein and dynactin concentration, though their detailed distributions were distinct from that of the motor protein complexes (Fig. 2, d–f). In the well-spread lamellipodia of chick embryo fibroblasts, the region of dynein and dynactin enrichment was within the zone where the actin-rich lamellipodium encounters microtubule ends (Fig. 2, p–r and not depicted). No apparent colocalization between dynein and the focal adhesion protein vinculin could be detected (Fig. 2, g–i). Of considerable interest, LIS1 exhibited virtually the same pattern as dynein and dynactin throughout the leading edge of wounded NIH3T3 cell monolayers (Fig. 2, j–l), as it does in the cell cortex of mitotic epithelial cells (Faulkner et al., 2000).

In NIH3T3 cells, reorientation of the microtubule network occurs within 1–2 h of recovery from wounding (Gundersen and Bulinski, 1988; Palazzo et al., 2001). Both dynein and dynactin were enriched at the leading edge after 20 min of recovery, though staining appeared to increase steadily for several hours afterward. Thus, dynein and dynactin were present early enough at the leading cell edge to mediate reorientation of the microtubule network though why they continued to accumulate subsequently was uncertain.

Leading edge dynein and dynactin staining were absent in serum-starved cells (Fig. 3 a), which exhibit neither reorientation of the microtubule network nor cell migration (Gundersen et al., 1994; Palazzo et al., 2001). Serum addition triggers orientation of the microtubule network (Palazzo et al., 2001) and restored leading edge dynein staining (Fig. 3 b, arrows).

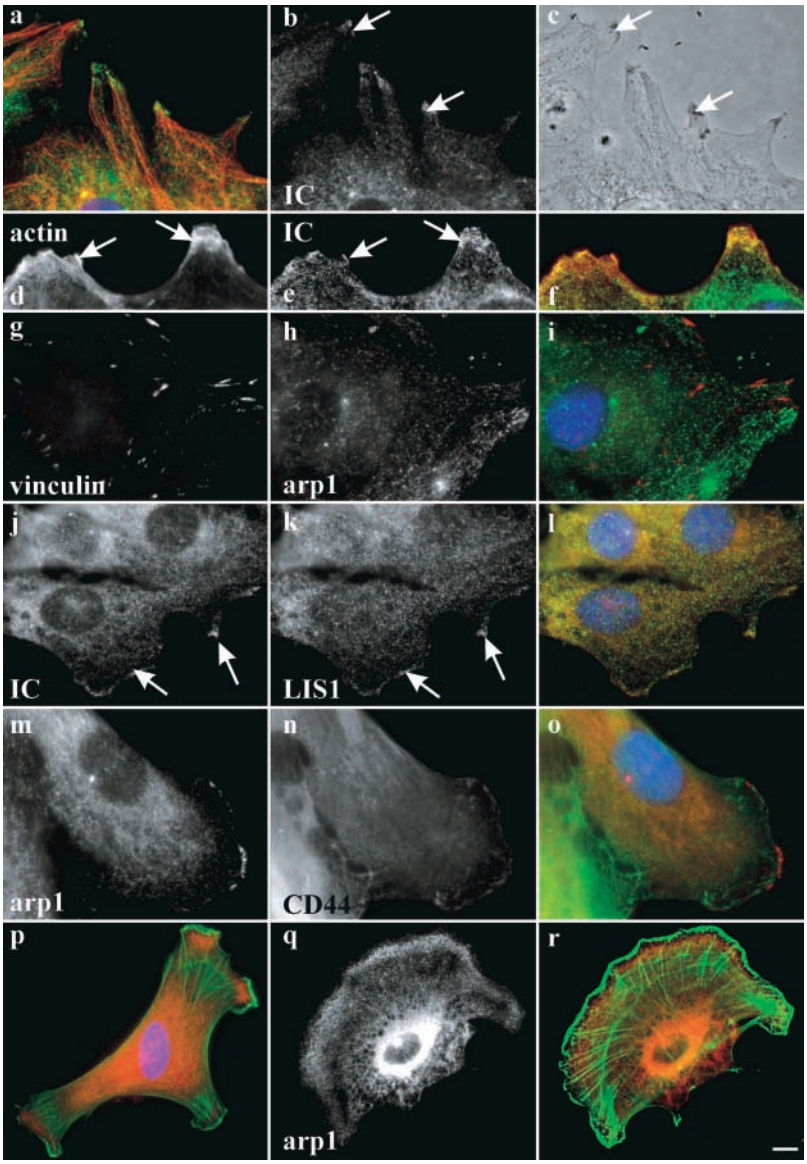

Figure 2. **Relative distribution of dynein and dynactin to other cell markers.** Immunofluorescence microscopy of wounded NIH3T3 cell monolayers (a–o) and chicken embryo fibroblasts (p–r). (a–c) Enrichment of dynein IC at the leading edge (arrows) of cells at regions of lamellipodial protrusion. (a) Immunofluorescence microscopy showing antitubulin (red) and antidynein IC (green); (b) antidynein IC alone; (c) phase contrast. (d–f) Distribution of dynein (e, green in f) versus actin (d, red in f). Dynein is enriched at these sites, but not coincident with actin (p–r). (g–i) Distribution of dynactin (h, green in i) versus vinculin (g, red in i). No clear evidence for colocalization is observed. (j and k) Distribution of dynein (j, green in l) versus LIS1 (k, red in l). Colocalization at sites throughout the leading edge is observed. (m–o) Distribution of dynactin (m, red in o) versus CD44 (n, green in o). The distributions of dynactin and CD44, which is enriched in membrane ruffles (not depicted), are distinct. (p–r) Relative distribution of dynactin (q, red in p and r) versus actin (green in p and r) in low density culture of chick embryo fibroblasts. Dynectin is diffusely enriched internal to actin. Cells in a–c were fixed 8 h, in d–l 1 h, and in m–o 6 h after wounding, respectively. Bar: (a–o) 5 μm; (p–r) 10 μm.

Localization of dynein by TIRF microscopy

Reorientation of the microtubule network can be induced without lamellipodial protrusion by use of lysophosphatidic acid (LPA; Palazzo et al., 2001). Surprisingly, leading edge staining was not clearly detected in LPA (Fig. 3 c). Similar results were obtained in the presence of serum plus cytochalasin D, which also allows for reorientation of the microtubule network without forward cell movement (Nagasaki et al., 1992; Palazzo et al., 2001). To determine whether lower levels of dynein and dynactin could be involved in the reorientation process, we used TIRF microscopy, which increases the detectability at the base of the cells due to the high signal to noise ratio achieved by this system. Staining was considerably more punctate than observed by epifluorescence. In the presence of serum, spots could be clearly observed enriched at the leading edge relative to other cell regions in close contact with the substratum (Fig. 3, d–o; Fig. S2, A and B, available at http://www.jcb.org/cgi/content/full/jcb.200310097/DC1), and many of them were associated with microtubules (Fig. 3, d–f, m, and n, arrows). Similar staining was observed after treatment with cytochalasin D (Fig. 3 o) or induction by LPA (Fig. 3, j–n), indicating that dynein is indeed present at the leading edge in conditions allowing for MTOC reorientation. In these cases, striking spots of dynein and dynactin could be observed at microtubule ends (Fig. 3, m and n, arrowheads). Leading edge enrichment was not clearly observed by TIRF microscopy in serum-starved cells (Fig. S2). We note that the number of spots and, therefore, the overall intensity of staining were higher at the leading edge of serum-stimulated cells, making the enrichment of dynein and dynactin at the leading edge more readily apparent in the presence of serum (Figs. 1 and 2 and Fig. 3 e).

Inhibition of directed cell movement

The appearance of the bright, diffuse leading edge dynein and dynactin staining pattern in the presence of serum, which alone allows for forward cell migration during wound healing, suggested a potential novel role for the motor protein in this process. To test this possibility, we overexpressed

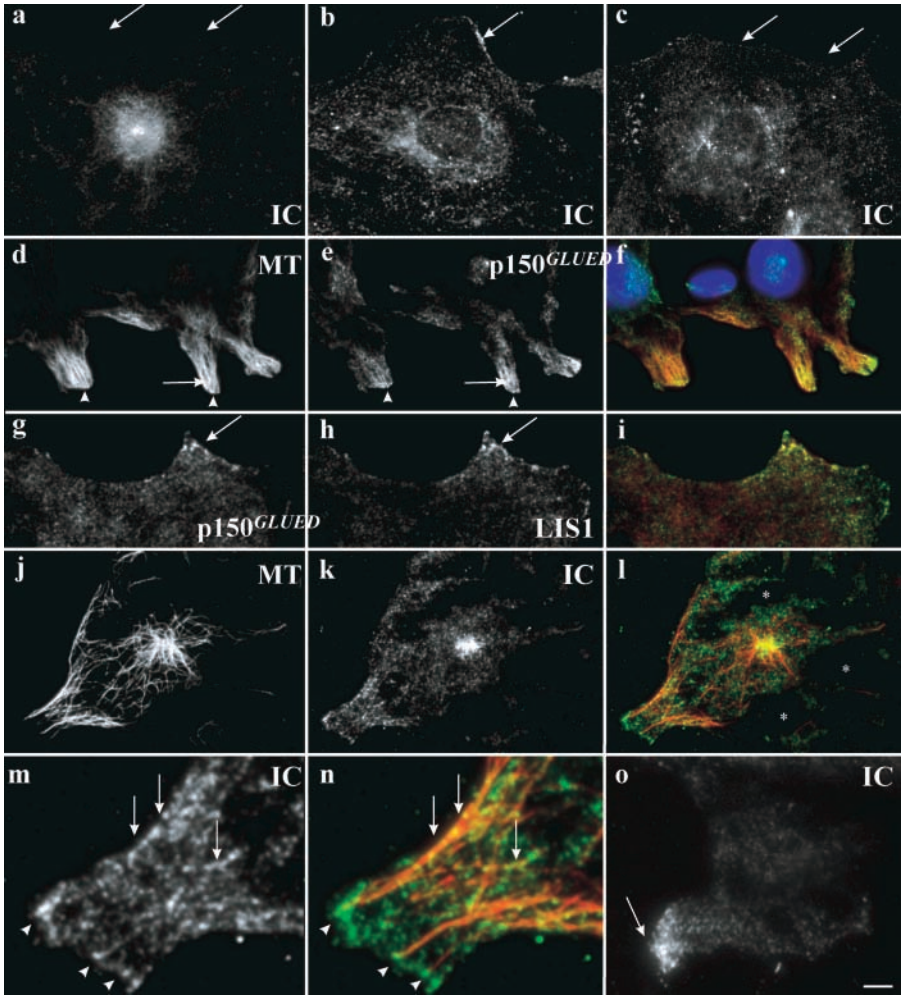

Figure 3. **Epifluorescence and TIRF microscopy during early times of wound healing.** (a–c) Immunofluorescence microscopy of dynein in (a) serum-starved cells at wound edge (arrows); (b) 2 h after serum addition; (c) 2 h after LPA addition. (d–i) TIRF microscopy of serum-grown cells 1 h after wounding stained with (d) antitubulin; (e) antidynactin ($p150^{GLUED}$); (f) merge ($p150^{GLUED}$, green; DAPI staining, blue); (g) antidynactin ($p150^{GLUED}$); (h) anti-LIS1; and (i) merge (LIS1, green). (j–n) TIRF microscopy of serum-starved cells exposed to LPA for 45 min stained with (j) antitubulin; (k) antidynein; (l) merge (dynein, green); (m) increased magnification of k; (n) increased magnification of l. (o) TIRF microscopy of serum-grown cells exposed to cytochalasin D for 45 min stained with antidynein. Bar: (d–f) 7 μm; (a–c, g–l, and o) 5 μm; (m and n) 2 μm.

a GFP tagged version of the dynamitin subunit of dynactin, which was shown to inhibit dynein function and block microtubule network orientation (Echeverri et al., 1996; Burkhardt et al., 1997; Palazzo et al., 2001; Dohner et al., 2002; though see Deacon et al., 2003). Overexpressing cells showed a marked decrease in motility (Fig. 4, A and D), and fell behind the wound edge during recovery (Fig. 4 C; Video 1, available at http://www.jcb.org/cgi/content/full/jcb.200310097/DC1). A similar effect was also produced by overexpressing cDNA encoding the NH_2-terminal portion of LIS1 (Fig. 4, C and D), which produced a pronounced mitotic phenotype without affecting the distribution of Golgi elements (Tai et al., 2002). We also injected cells with the well-characterized 70.1 mAb to the cytoplasmic dynein intermediate chains, which inhibits dynein function (Burkhardt et al., 1997; Faulkner et al., 2000; Yvon et al., 2001). Cells were injected with the antibody 2 h after wounding, sufficient time for centrosome orientation to have occurred (Palazzo et al., 2001). The cells were followed by time lapse microscopy and subsequently fixed for immunofluorescence. Again, migration was less efficient compared with controls (Fig. 4 C). In all three cases the rate of migration was clearly decreased (Fig. 4 D). Although ruffling activity and lamellipodial protrusion persisted in most cells, these activities were clearly abolished or reduced in 36% of dynein inhibited cells (Videos 1 and 2, available at http://www.jcb.org/cgi/content/full/jcb.200310097/DC1).

To test for other possible effects on cytoplasmic dynein function, the organization of the Golgi apparatus was examined 4 h after the 70.1 antibody was injected. The Golgi apparatus remained condensed in the perinuclear region in 89% of the injected cells ($n = 55$) versus 92% of noninjected controls ($n = 48$; Fig. S2 C), a result comparable to the insensitivity of the Golgi apparatus to this antibody during microtubule reorientation at short times of wound healing (Palazzo et al., 2001). However, the Golgi apparatus remained oriented toward the leading edge in most (76%; $n = 55$) of the injected cells, similar to control cells (84%; $n = 51$).

Model for leading edge dynein function

Our results reveal an enrichment of dynein, dynactin, and LIS1 at the leading cell edge during wound recovery in what appear to be two distinct subcellular pools, potentially involved in two distinct functions. The punctate staining observed along microtubules and at microtubule ends is observed during the early phase of the wound healing process and under conditions that support the reorientation of the microtubule network but do not stimulate migration. The punctate structures appear to represent sites of attachment

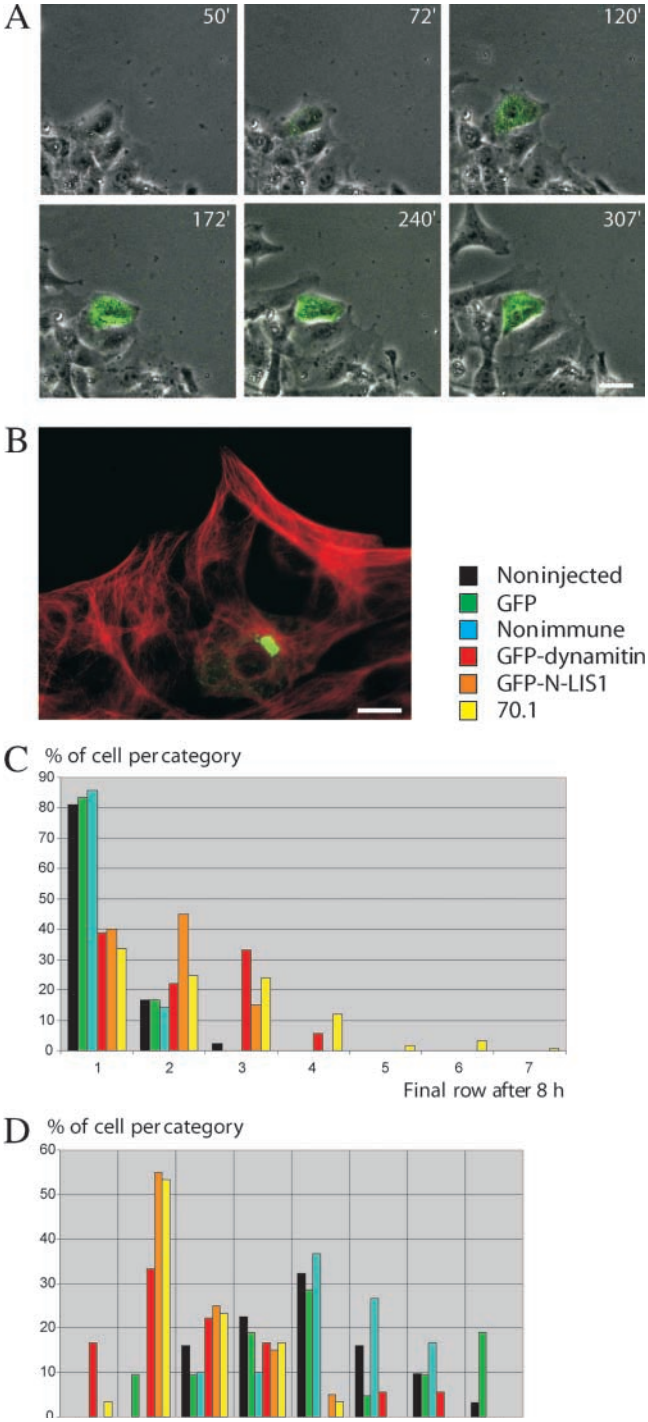

Figure 4. **Inhibition of dynein, dynactin, and LIS1 function interferes with cell migration.** (A) Dual fluorescent and phase-contrast time lapse microscopy of cells wounded in the presence of serum. One cell in the field was injected with a plasmid encoding GFP-dynamitin, which was detectable as a green fluorescing signal by 60 min after injection. This cell gradually fell behind others at the wound edge. Numbers refer to minutes after wounding. (B) A monolayer of cells was wounded in the presence of serum and injected with anti-IC antibody 2 h later. After 8 h, the cells were fixed and the level of injected antibody was confirmed by immunofluorescence microscopy (antidynein antibody in green, antitubulin in red). The injected cell was seen to have fallen behind the uninjected cells at the wound edge. (C) Effects of inhibitory cDNAs and antibody on final cell position. Cell row number was determined 8 h after antibody injection or injection of inhibitory cDNA. GFP-dynamitin (red bars) and GFP-LIS1-N (orange bars) overexpressing cells as well as antidynein-injected cells (yellow bars) fell back from the leading wound edge. $n = 42$ (noninjected), 63 (nonimmune injected), 24 (GFP), 77 (antibody injected), 18 (GFP-dynamitin), and 20 (GFP-LIS1). (D) Distribution of speeds. The median speed was reduced by the inhibitory agents to 50–100 nm/min relative to the control values of 200–250 nm/min. Mean speeds were: GFP-dynamitin (121 ± 75 nm/min; $n = 18$); GFP-LIS1-N (113 ± 42 nm/min; $n = 20$); and antidynein injected cells (107 ± 46 nm/min; $n = 30$). These values were significantly lower than mean control speeds (t tests, $P < 0.01$): noninjected cells (227 ± 76 nm/min; $n = 31$); GFP overexpressors (231 ± 91 nm/min; $n = 21$); and nonimmune serum-injected cells (238 ± 61 nm/min; $n = 30$). Bars: (A) 20 μm; and (B) 10 μm.

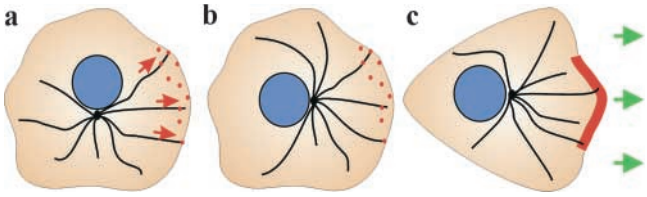

Figure 5. **Role of cytoplasmic dynein and its associated proteins during wound healing.** (a and b) Cytoplasmic dynein is shown at punctate sites (red spots) at the leading cell cortex during reorientation of the microtubule network. Dynein and its associated proteins are proposed to pull on microtubules from these sites (red arrows) and/or anchor the microtubule network against retrograde forces. (c) During cell migration, dynein is enriched in regions of lamellipodial protrusion where it is proposed to regulate forward cell movement (green arrows).

between microtubules and cortical dynein, and may represent the loci at which dynein pulls on microtubules to reorient the microtubule network and associated organelles (Fig. 5). Cortical dynein has been detected in different systems (for review see Dujardin and Vallee, 2002). Dynein and dynactin have been identified at the cell cortex in dividing cells where they orient the mitotic spindle through its astral microtubules (Busson et al., 1998; Faulkner et al., 2000). How this dynein pool may be related to that reported in the current paper is uncertain. Dynein and dynactin have also have been implicated in the reorientation of the centrosome–nucleus complex in two-cell stage *Caenorhabditis elegans* embryos, where they may act either from the site of the midbody from the prior cell division or from the region of the cortex lying between the two cells (for review see Dujardin and Vallee, 2002). Dynein has been phenotypically implicated in maintaining centrosome position during interphase in amoeboid and nonmotile epithelial cells (Koonce et al., 1999; Burakov et al., 2003), a potentially related phenomenon, though the sites from which dynein may act in these cases were not determined. Spots of dynein or its regulatory proteins have also been seen at the tips of microtubules reaching the cortex during meiotic nuclear oscillations in *Schizosaccharomyces pombe* (Yamamoto et al., 1999), in *Saccharomyces cerevisiae* buds (Lee et al., 2003; Sheeman et al., 2003), and at the hyphal tip of filamentous fungi (Xiang et al., 1995; Minke et al., 1999). Dynein and dynactin have been localized to other cortical sites, such as adherens junctions (Ligon et al., 2001). These structures are absent from

the leading edge of the migrating fibroblasts used in our paper, and, therefore, unlikely to be responsible for the currently observed leading edge localization. Furthermore, although microtubules interact with focal adhesions (Kaverina et al., 1998), this behavior was found to involve kinesin rather than dynein (Krylyshkina et al., 2002).

The bright, more diffuse staining we observe at the leading edge of migrating fibroblasts is detectable in the early stages of wound healing, but continues to accumulate during the subsequent phase of cell migration, and is abolished by conditions that interfere with this latter process. These observations support an additional novel role for dynein in cell translocation. This possibility was confirmed by use of dynamitin and LIS1 overexpression, as well as dynein antibody injection. Dynein and dynactin were enriched within regions of lamellipodial protrusion. Because dynein is only known to produce force in conjunction with microtubules, our observations supports the existence of a novel pool of dynein associated with the actin-rich cortical cytoskeleton which could be available for capture of microtubules entering this region.

Interference with cytoplasmic dynein, dynactin, or LIS1 resulted in decreased cell migration, revealing a persistent requirement for dynein and its regulatory proteins in forward migration. Limited microtubule depolymerization also inhibits forward cell movement in this assay (Liao et al., 1995), and there may well be a common physiological basis for these responses. To determine whether the migration defects produced by dynein inhibitors resulted from effects on the orientation of the microtubule cytoskeleton, we allowed wound healing to proceed for 2 h before injecting antidynein antibody. Forward cell migration was inhibited despite the completion of the microtubule reorientation phase of the wound healing process. No change in the orientation of the Golgi apparatus was observed. This observation indicates that an important component of the cell's biosynthetic machinery remained oriented toward the leading cell edge, and suggested that the same was true for the microtubule organizing center. Thus, inhibition of cell migration does not appear to involve disruption of the microtubule cytoskeleton and may involve a distinct and novel dynein function.

What precisely this function may be remains to be fully elucidated. Recent evidence has revealed a retrograde flux of actin filaments toward the cell center from the leading lamellipodium in migrating cells, which produces a backward force on microtubules and, presumably, their associated organelles (Salmon et al., 2002). Leading edge dynein might potentially serve as a holdfast for those microtubules which invade the actin network at the front of the cell. Consistent with this hypothesis, bidirectional, actomyosin-mediated movements of microtubules in PtK2 cells were enhanced by dynein inhibition (Yvon et al., 2001).

It is also possible that the link of leading edge microtubules to cortical cytoplasmic dynein serves as a means of communication between the microtubule and actin cytoskeleton. As envisaged for cortical dynein, kinetochore dynein interacts with the plus ends of microtubules. From this site, it both pulls on chromosomes and removes checkpoint proteins (Howell et al., 2001), regulating cell cycle progression. Conceivably, tension produced through the interaction of microtubules with cortical dynein could serve to regulate actin based motility, through a tension sensing or other signaling mechanism. The activation of lamellipodial protrusion by microtubule growth (Waterman-Storer et al., 1999), and the recent finding that LIS1 haploinsufficiency affects filamentous actin organization at the leading edge (Kholmanskikh et al., 2003) are potentially consistent with this hypothesis.

Type I lissencephaly, which is caused by mutations in the human *LIS1* gene, is thought to involve a defect in the migration of differentiating neurons in the developing brain (for review see Morris, 2000). This possibility is supported by an effect of reduced LIS1 expression on nuclear movements within cerebellar granule reaggregate cultures (Hirotsune et al., 1998; Kholmanskikh et al., 2003), and free translocation of brain derived fibroblasts (Kholmanskikh et al., 2003). Based on evidence for the codistribution of LIS1 with dynein at kinetochores and the mitotic cell cortex, as well as a pronounced LIS1 mitotic phenotype, we have suggested a role for LIS1 in the timing and orientation of progenitor cell divisions (Vallee et al., 2000). The finding of LIS1 at the leading edge of the migrating cells in the current paper identifies a new site for dynein and LIS1 colocalization. Inhibition of cell migration by a dominant negative LIS1 fragment supports a dynein regulatory role this site. Further work will be directed at testing this possibility.

Materials and methods

Cell culture and live cell imaging

NIH3T3 fibroblasts were grown to confluence in the presence or absence of bovine calf serum (Palazzo et al., 2001) and treated with 0.25 μM cytochalasin D or 1 μM LPA as required (Palazzo et al., 2001). GFP-dynamitin and GFP-LIS1-N cDNAs (Palazzo et al., 2001; Dohner et al., 2002; Tai et al., 2002), or monoclonal antidynein intermediate chain antibody concentrated at 18–20 mg/ml (clone 70.1; Sigma-Aldrich) were injected, respectively, in the nucleus and the cytoplasm using a semi-automatic microinjector (Eppendorf) as described previously (Faulkner et al., 2000). Primary chick embryo fibroblasts were prepared from E10 embryos and grown in sparse culture in medium 199 (Sigma-Aldrich) supplemented with 5% FCS and 1% chicken serum on fibronectin-coated coverslips. Live cells were recorded at 37°C in a 5% CO_2 atmosphere using inverted microscopes (model DMIRBE; Leica) equipped with an incubation chamber. Images were collected with a CCD camera (model ORCA 100; Hamamatsu) piloted by Metamorph (Universal Imaging Corp.), or a CCD camera (model DC F350; Leica) piloted by the Leica FW4000 software. Confocal pictures were acquired on a confocal microscope (model MRC1024; Bio-Rad Laboratories). TIRF images were collected using a microscope (model Eclipse TE2000-u; Nikon) with a Turnkey TIRF module. Images were processed using Metamorph and Photoshop softwares.

Immunocytochemistry and immunological reagents

Cells were fixed after wounding by immersion in −20°C methanol for 6 min, or 20 min in 3% PFA (Fig. 2, j–l and Fig. 3, g–i) followed by 1 h incubations in primary and secondary antibodies diluted in PBS containing 0.05% BSA. Antibodies included polyclonal antidynein IC (Vaughan et al., 1999), anti-CD44 (Perschl et al., 1995), anti-p150^{GLUED}, and anti-GM130 (Transduction Labs), antitubulin (DM1A), -actin (AC-40), and -vinculin (all from Sigma-Aldrich), monoclonal anti-LIS1 (provided by O. Reiner, Weizmann Institute, Rehovot, Israel), polyclonal anti-IQGAP1 (provided by G. Bloom, University of Virginia, Charlottesville, VA), polyclonal anti–Arp-1 (provided by D. Meyer, University of California, Los Angeles, Los Angeles, CA), Alexa green–conjugated secondary antibodies (Molecular Probes Inc.), and Cy3- and Cy5-conjugated secondary antibodies (Jackson ImmunoResearch Laboratories).

Online supplemental material

Two videos illustrating NIH3T3 cell migration defects after dynein inhibition. Video 1 shows cell migration after overexpression of GFP-dynamitin,

and Video 2 shows cell migration after injection with antidynein antibody. Two additional figures are also provided. Fig. S1 shows the distribution of dynein relative to membrane ruffles, as well as the quantification of dynein enrichment at the leading edge. Fig. S2 shows that dynein is enriched at the leading edge using TIRF microscopy, as well as the normal distribution of the Golgi apparatus after injection of antidynein antibodies. Online supplemental material is available at http://www.jcb.org/cgi/content/full/jcb.200310097/DC1.

We thank Drs. Orly Reiner, David Meyer, and George Bloom for antibody reagents; Yu Chen, Anna Kalinovsky, and Célia Clouet for technical contributions; and Dr. Jan De Mey for the use of microscopy equipment in the later stages of this project.

This work was supported by grants to R.B. Vallee (NIH GM47434 and HD61982, and a March of Dimes Birth Defects Foundation grant); to G.G. Gundersen (NIH GM62939); and to D.L. Dujardin (Human Frontiers Science Program Fellowship).

Submitted: 20 October 2003
Accepted: 13 November 2003

References

Burakov, A., E. Nadezhdina, B. Slepchenko, and V. Rodionov. 2003. Centrosome positioning in interphase cells. *J. Cell Biol.* 162:963–969.

Burkhardt, J.K., C.J. Echeverri, T. Nilsson, and R.B. Vallee. 1997. Overexpression of the dynamitin (p50) subunit of the dynactin complex disrupts dynein-dependent maintenance of membrane organelle distribution. *J. Cell Biol.* 139:469–484.

Busson, S., D. Dujardin, A. Moreau, J. Dompierre, and J.R. De Mey. 1998. Dynein and dynactin are localized to astral microtubules and at cortical sites in mitotic epithelial cells. *Curr. Biol.* 8:541–544.

Deacon, S.W., A.S. Serpinskaya, P.S. Vaughan, M. Lopez Fanarraga, I. Vernos, K.T. Vaughan, and V.I. Gelfand. 2003. Dynactin is required for bidirectional organelle transport. *J. Cell Biol.* 160:297–301.

Dohner, K., A. Wolfstein, U. Prank, C. Echeverri, D. Dujardin, R. Vallee, and B. Sodeik. 2002. Function of dynein and dynactin in herpes simplex virus capsid transport. *Mol. Biol. Cell.* 13:2795–2809.

Dujardin, D.L., and R.B. Vallee. 2002. Dynein at the cortex. *Curr. Opin. Cell Biol.* 14:44–49.

Echeverri, C.J., B.M. Paschal, K.T. Vaughan, and R.B. Vallee. 1996. Molecular characterization of the 50-kD subunit of dynactin reveals function for the complex in chromosome alignment and spindle organization during mitosis. *J. Cell Biol.* 132:617–633.

Etienne-Manneville, S., and A. Hall. 2001. Integrin-mediated activation of Cdc42 controls cell polarity in migrating astrocytes through PKCzeta. *Cell.* 106: 489–498.

Faulkner, N.E., D.L. Dujardin, C.Y. Tai, K.T. Vaughan, C.B. O'Connell, Y. Wang, and R.B. Vallee. 2000. A role for the lissencephaly gene LIS1 in mitosis and cytoplasmic dynein function. *Nat. Cell Biol.* 2:784–791.

Gundersen, G.G., and J.C. Bulinski. 1988. Selective stabilization of microtubules oriented toward the direction of cell migration. *Proc. Natl. Acad. Sci. USA.* 85:5946–5950.

Gundersen, G.G., I. Kim, and C.J. Chapin. 1994. Induction of stable microtubules in 3T3 fibroblasts by TGF-beta and serum. *J. Cell Sci.* 107:645–659.

Hirotsune, S., M.W. Fleck, M.J. Gambello, G.J. Bix, A. Chen, G.D. Clark, D.H. Ledbetter, C.J. McBain, and A. Wynshaw-Boris. 1998. Graded reduction of Pafah1b1 (Lis1) activity results in neuronal migration defects and early embryonic lethality. *Nat. Genet.* 19:333–339.

Howell, B.J., B.F. McEwen, J.C. Canman, D.B. Hoffman, E.M. Farrar, C.L. Rieder, and E.D. Salmon. 2001. Cytoplasmic dynein/dynactin drives kinetochore protein transport to the spindle poles and has a role in mitotic spindle checkpoint inactivation. *J. Cell Biol.* 155:1159–1172.

Kaverina, I., K. Rottner, and J.V. Small. 1998. Targeting, capture, and stabilization of microtubules at early focal adhesions. *J. Cell Biol.* 142:181–190.

Kholmanskikh, S.S., J.S. Dobrin, A. Wynshaw-Boris, P.C. Letourneau, and M.E. Ross. 2003. Disregulated RhoGTPases and actin cytoskeleton contribute to the migration defect in Lis1-deficient neurons. *J. Neurosci.* 23:8673–8681.

King, S.J., and T.A. Schroer. 2000. Dynactin increases the processivity of the cytoplasmic dynein motor. *Nat. Cell Biol.* 2:20–24.

Koonce, M.P., J. Kohler, R. Neujahr, J.M. Schwartz, I. Tikhonenko, and G. Gerisch. 1999. Dynein motor regulation stabilizes interphase microtubule arrays and determines centrosome position. *EMBO J.* 18:6786–6792.

Krylyshkina, O., I. Kaverina, W. Kranewitter, W. Steffen, M.C. Alonso, R.A. Cross, and J.V. Small. 2002. Modulation of substrate adhesion dynamics via microtubule targeting requires kinesin-1. *J. Cell Biol.* 156:349–359.

Lee, W.L., J.R. Oberle, and J.A. Cooper. 2003. The role of the lissencephaly protein Pac1 during nuclear migration in budding yeast. *J. Cell Biol.* 160:355–364.

Liao, G., T. Nagasaki, and G.G. Gundersen. 1995. Low concentrations of nocodazole interfere with fibroblast locomotion without significantly affecting microtubule level: implications for the role of dynamic microtubules in cell locomotion. *J. Cell Sci.* 108:3473–3483.

Ligon, L.A., S. Karki, M. Tokito, and E.L. Holzbaur. 2001. Dynein binds to beta-catenin and may tether microtubules at adherens junctions. *Nat. Cell Biol.* 3:913–917.

Minke, P.F., I.H. Lee, and M. Plamann. 1999. Microscopic analysis of Neurospora ropy mutants defective in nuclear distribution. *Fungal Genet. Biol.* 28:55–67.

Morris, R. 2000. A rough guide to a smooth brain. *Nat. Cell Biol.* 2:E201–E202.

Nagasaki, T., C.J. Chapin, and G.G. Gundersen. 1992. Distribution of detyrosinated microtubules in motile NRK fibroblasts is rapidly altered upon cell-cell contact: implications for contact inhibition of locomotion. *Cell Motil. Cytoskeleton.* 23:45–60.

Palazzo, A.F., H.L. Joseph, Y.J. Chen, D.L. Dujardin, A.S. Alberts, K.K. Pfister, R.B. Vallee, and G.G. Gundersen. 2001. Cdc42, dynein, and dynactin regulate MTOC reorientation independent of Rho-regulated microtubule stabilization. *Curr. Biol.* 11:1536–1541.

Perschl, A., J. Lesley, N. English, R. Hyman, and I.S. Trowbridge. 1995. Transmembrane domain of CD44 is required for its detergent insolubility in fibroblasts. *J. Cell Sci.* 108:1033–1041.

Reiner, O., R. Carrozzo, Y. Shen, M. Wehnert, F. Faustinella, W.B. Dobyns, C.T. Caskey, and D.H. Ledbetter. 1993. Isolation of a Miller-Dieker lissencephaly gene containing G protein beta-subunit-like repeats. *Nature.* 364:717–721.

Salmon, W.C., M.C. Adams, and C.M. Waterman-Storer. 2002. Dual-wavelength fluorescent speckle microscopy reveals coupling of microtubule and actin movements in migrating cells. *J. Cell Biol.* 158:31–37.

Sasaki, S., A. Shionoya, M. Ishida, M.J. Gambello, J. Yingling, A. Wynshaw-Boris, and S. Hirotsune. 2000. A LIS1/NUDEL/cytoplasmic dynein heavy chain complex in the developing and adult nervous system. *Neuron.* 28:681–696.

Sheeman, B., P. Carvalho, I. Sagot, J. Geiser, D. Kho, M.A. Hoyt, and D. Pellman. 2003. Determinants of *S. cerevisiae* dynein localization and activation. Implications for the mechanism of spindle positioning. *Curr. Biol.* 13:364–372.

Smith, D.S., M. Niethammer, R. Ayala, Y. Zhou, M.J. Gambello, A. Wynshaw-Boris, and L.H. Tsai. 2000. Regulation of cytoplasmic dynein behaviour and microtubule organization by mammalian Lis1. *Nat. Cell Biol.* 2:767–775.

Tai, C.Y., D.L. Dujardin, N.E. Faulkner, and R.B. Vallee. 2002. Role of dynein, dynactin, and CLIP-170 interactions in LIS1 kinetochore function. *J. Cell Biol.* 156:959–968.

Vallee, R.B., N.E. Faulkner, and C.Y. Tai. 2000. The role of cytoplasmic dynein in the human brain developmental disease lissencephaly. *Biochim. Biophys. Acta.* 1496:89–98.

Vaughan, K.T., S.H. Tynan, N.E. Faulkner, C.J. Echeverri, and R.B. Vallee. 1999. Colocalization of cytoplasmic dynein with dynactin and CLIP-170 at microtubule distal ends. *J. Cell Sci.* 112:1437–1447.

Waterman-Storer, C.M., R.A. Worthylake, B.P. Liu, K. Burridge, and E.D. Salmon. 1999. Microtubule growth activates Rac1 to promote lamellipodial protrusion in fibroblasts. *Nat. Cell Biol.* 1:45–50.

Xiang, X., C. Roghi, and N.R. Morris. 1995. Characterization and localization of the cytoplasmic dynein heavy chain in *Aspergillus nidulans*. *Proc. Natl. Acad. Sci. USA.* 92:9890–9894.

Yamamoto, A., R.R. West, J.R. McIntosh, and Y. Hiraoka. 1999. A cytoplasmic dynein heavy chain is required for oscillatory nuclear movement of meiotic prophase and efficient meiotic recombination in fission yeast. *J. Cell Biol.* 145:1233–1249.

Yvon, A.M., D.J. Gross, and P. Wadsworth. 2001. Antagonistic forces generated by myosin II and cytoplasmic dynein regulate microtubule turnover, movement, and organization in interphase cells. *Proc. Natl. Acad. Sci. USA.* 98: 8656–8661.